Two mechanisms of remote synchronization in a chain of Stuart-Landau oscillators

Mohit Kumar [*]
Department of Mechanical Engineering, Indian Institute of Technology Madras, Chennai 600036, India

Michael Rosenblum [†]
Department of Physics and Astronomy, University of Potsdam, Karl-Liebknecht-Strasse 24/25, D-14476 Potsdam-Golm, Germany

(Received 31 August 2021; accepted 14 October 2021; published 8 November 2021)

Remote synchronization implies that oscillators interacting not directly but via an additional unit (hub) adjust their frequencies and exhibit frequency locking while the hub remains asynchronous. In this paper, we analyze the mechanisms of remote synchrony in a small network of three coupled Stuart-Landau oscillators using recent results on higher-order phase reduction. We analytically demonstrate the role of two factors promoting remote synchrony. These factors are the nonisochronicity of oscillators and the coupling terms appearing in the second-order phase approximation. We show a good correspondence between our theory and numerical results for small and moderate coupling strengths.

DOI: 10.1103/PhysRevE.104.054202

I. INTRODUCTION

Remote synchrony (RS) is an interesting manifestation of the general and highly significant nonlinear phenomenon of synchronization [1]. RS implies adjusting rhythms of oscillators that do not interact directly but only through an asynchronous unit (hub). The effect was briefly reported by Okuda and Kuramoto as early as 1991; observation of an indirect synchronization of several oscillators was a by-product of their detailed analysis of interacting oscillator populations [2]. A more recent paper by Bergner *et al.* [3] stimulated interest in exploring RS through numerical and experimental studies [4]. Understanding RS is crucial, e.g., for the interpretation of functional connectivity in brain networks [5,6].

Previous studies analyzed RS in starlike and complex networks of Stuart-Landau (SL) or phase oscillators [3,4,6,7]. The results uncovered the role of amplitude dynamics [3,7]: RS appeared in a network of isochronous SL units but not in its first-order phase approximation, i.e., in the Kuramoto network. Furthermore, Vlasov and Bifone [6] demonstrated that RS emerges in networks of phase oscillators with the Kuramoto-Sakaguchi interaction [8], but not in the case of zero phase shift in the sine-coupling term. Since the Kuramoto-Sakaguchi model is the first-order approximation of coupled nonisochronous SL oscillators, this result indicates the role of nonisochronicity in promoting RS. However, the understanding of mechanisms leading to RS is yet incomplete. This paper uses a simple motif of three coupled SL oscillators to analyze the transition to RS. In contradistinction to Ref. [6], we consider nonidentical peripheral oscillators. Using recent results on higher-order phase reduction [9], we explain the contribution of both the nonisochronicity and the amplitude dynamics and quantitatively describe the transition to RS. We demonstrate the importance of higher-order phase approximation in the explanation of RS.

The paper is organized as follows. In Sec. II, we introduce the model and its second-order phase approximation. Next, we demonstrate the transition to RS in this model. In Sec. III, we derive the condition for this transition, and in Sec. IV, we present our results. Section V concludes and discusses our findings.

II. REMOTE SYNCHRONY IN COUPLED STUART-LANDAU OSCILLATORS

Consider three SL oscillators coupled in a chain as $1 \leftrightarrows 2 \leftrightarrows 3$. Thus, peripheral units 1 and 3 are not interacting directly but only through the central oscillator. Let the (generally different) natural frequencies of the oscillators be $\omega_{1,2,3}$. Correspondingly, we denote the frequencies of interacting units (observed frequencies) as $\Omega_{1,2,3}$. Following Bergner *et al.* [3], we say that the network reaches a state of RS if with an increase in coupling strength Ω_1 becomes equal to Ω_3 whereas $\Omega_1 \neq \Omega_2$. If all frequencies coincide, $\Omega_1 = \Omega_2 = \Omega_3$, then we speak about complete synchrony (CS). We emphasize that Refs. [10] use the term RS in a different context.

In the rest of this section, we first specify our model and present its second-order phase approximation. Next, we numerically demonstrate transitions from asynchrony to RS and CS in the full model and its phase-reduced versions.

A. Model and its phase approximation

The governing equations of the model are as follows:

$$\dot{A}_n = [1 + i(\omega_n + \alpha)]A_n - (1 + i\alpha)|A_n|^2 A_n + \varepsilon I_n, \qquad (1)$$

where $A_n \in \mathbb{C}$, $n = 1, 2, 3$, ω_n is the natural frequency of the nth oscillator, and α is the nonisochronicity parameter,

[*] mohitkumar.2k1@gmail.com
[†] mros@uni-potsdam.de

common for all units. The parameter ε and the terms $I_1 = A_2,\ I_2 = A_1 + A_3,\ I_3 = A_2$ describe the strength and structure of the coupling, respectively. We emphasize that the form of the governing equation ensures the independence of autonomous frequencies on nonisochronicity α [11].

It is well known that for sufficiently weak coupling, the dynamics of interacting limit-cycle oscillators reduce to that of phases. For the coupled SL oscillators, the first-order phase approximation in ε can be performed analytically because the phase of this system can be readily obtained from the state variable A; the reduction yields the celebrated Kuramoto-Sakaguchi phase equations [8]. However, phase reduction beyond the first-order approximation remains challenging and is a subject of ongoing research. Here, we use the results of Gengel *et al.* [9], who provided expressions for the second-order reduction of coupled SL oscillators [12]. Let the phase of the nth oscillator be φ_n. The second-order phase approximation of the system (1) reads

$$\begin{aligned}
\dot{\varphi}_1 &= \omega_1 + \varepsilon[\sin(\varphi_2-\varphi_1) - \alpha\,\cos(\varphi_2-\varphi_1)] + \varepsilon^2[D_{32}\cos(2\varphi_2-\varphi_1-\varphi_3) + C_{32}\sin(2\varphi_2-\varphi_1-\varphi_3)\\
&\quad - D_{32}\cos(\varphi_3-\varphi_1) + C_{32}\sin(\varphi_3-\varphi_1)] + O(\varepsilon^3),\\
\dot{\varphi}_2 &= \omega_2 + \varepsilon[\sin(\varphi_1-\varphi_2) - \alpha\,\cos(\varphi_1-\varphi_2) + \sin(\varphi_3-\varphi_2) - \alpha\,\cos(\varphi_3-\varphi_2)]\\
&\quad + \varepsilon^2[(D_{12}+D_{32})\cos(2\varphi_2-\varphi_1-\varphi_3) + (C_{12}+C_{32})\sin(2\varphi_2-\varphi_1-\varphi_3)\\
&\quad - (D_{12}+D_{32})\cos(\varphi_1-\varphi_3) + (C_{12}-C_{32})\sin(\varphi_1-\varphi_3)] + O(\varepsilon^3),\\
\dot{\varphi}_3 &= \omega_3 + \varepsilon[\sin(\varphi_2-\varphi_3) - \alpha\,\cos(\varphi_2-\varphi_3)] + \varepsilon^2[D_{12}\cos(2\varphi_2-\varphi_3-\varphi_1) + C_{12}\sin(2\varphi_2-\varphi_3-\varphi_1)\\
&\quad - D_{12}\cos(\varphi_1-\varphi_3) + C_{12}\sin(\varphi_1-\varphi_3)] + O(\varepsilon^3),
\end{aligned} \tag{2}$$

where

$$C_{ij} = \frac{1+\alpha^2}{4+(\omega_i-\omega_j)^2}, \tag{3}$$

and

$$D_{ij} = \frac{1+\alpha^2}{2}\left(\frac{\omega_i-\omega_j}{4+(\omega_i-\omega_j)^2}\right). \tag{4}$$

Keeping in Eq. (2) only the first-order terms $\sim\varepsilon$, one obtains the Kuramoto-Sakaguchi model,

$$\begin{aligned}
\dot{\varphi}_1 &= \omega_1 + \varepsilon[\sin(\varphi_2-\varphi_1) - \alpha\,\cos(\varphi_2-\varphi_1)],\\
\dot{\varphi}_2 &= \omega_2 + \varepsilon[\sin(\varphi_1-\varphi_2) - \alpha\,\cos(\varphi_1-\varphi_2)\\
&\quad + \sin(\varphi_3-\varphi_2) - \alpha\,\cos(\varphi_3-\varphi_2)],\\
\dot{\varphi}_3 &= \omega_3 + \varepsilon[\sin(\varphi_2-\varphi_3) - \alpha\,\cos(\varphi_2-\varphi_3)].
\end{aligned} \tag{5}$$

For isochronous oscillators $\alpha = 0$, the model simplifies to the Kuramoto network.

B. Remote synchrony in the full and reduced models

This section compares and contrasts the regions of RS obtained using the SL system (1) and the phase approximations, see Eqs. (5) and (2). To this end, we fix the natural frequencies of all three oscillators [13], numerically simulate the governing equations, and detect regions of asynchrony, CS, and RS upon varying the coupling strength and the nonisochronicity parameter. (The description of the numerical procedures are deferred to Sec. IV.) This results in two-parameter bifurcation diagrams on the ε-α plane shown in Fig. 1.

Figure 1 provides us with two insights. First, we note that the first-order approximation does not accurately reproduce the transition to RS. This approximation's failure results from not accounting for the amplitude modulation in the coupled SL oscillators. On the other hand, the second-order approximation fares well and is accurate for small and moderate coupling strengths. Second, the nonisochronicity parameter essentially affects the transition to RS. Generally, RS in the SL system (1) appears for both the isochronous ($\alpha = 0$) and the nonisochronous ($\alpha \neq 0$) cases. However, this feature is captured only by the second-order approximation; the first approximation does not exhibit RS for $\alpha = 0$, in agreement with the results by Vlasov and Bifone [6].

III. THEORETICAL ANALYSIS OF THE PHASE DYNAMICS

We use the phase equations (2) to investigate the transition to RS. It is straightforward to reduce Eqs. (2) to a

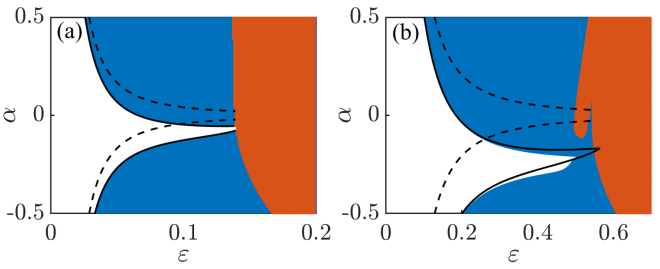

FIG. 1. Numerically computed bifurcation diagrams illustrating the dependence of the system's observed state on the coupling strength ε and nonisochronicity parameter α. The oscillators' natural frequencies are (a) $\omega_1 = 1,\ \omega_2 = \sqrt{2},\ \omega_3 = 1.002$, and (b) $\omega_1 = 1,\ \omega_2 = \sqrt{7},\ \omega_3 = 1.01$. The white, blue (dark gray), and red (light gray) regions correspond to asynchrony, RS, and CS, respectively, upon numerical simulation of Eq. (1). The solid black line depicts the RS transition border as computed using the second-order phase approximation, see Eqs. (2). The dashed black line shows the RS transition obtained for the first-order phase approximation, see Eqs. (5). The diagrams demonstrate the crucial role of the nonisochronicity parameter α. Furthermore, the diagrams clearly show the advantage of the second-order approximation.

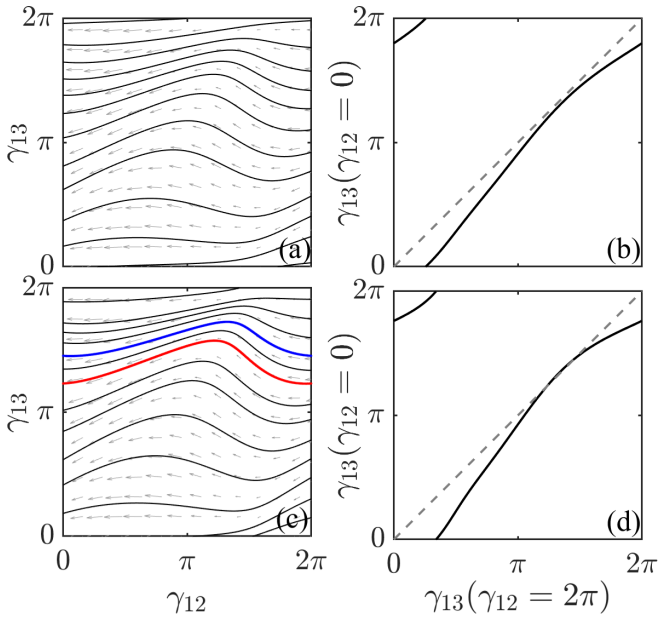

FIG. 2. Illustration of the RS transition using the phase approximation equations upon increasing the coupling strength. (a) and (c) Phase plane representations of the phase difference dynamics at low and moderate coupling strengths, respectively. The bold blue (dark gray) and red (light gray) trajectories in panel (c) depict the stable and unstable limit cycles. (b) and (d) Poincaré maps corresponding to the flows shown in panels (a) and (c), respectively, constructed using the Poincaré section $\gamma_{12} = 2\pi$. The birth of a stable limit cycle (fixed point) in the phase plane plot (Poincaré map) corresponds to the onset of RS. (The plots shown here are computed using the first-order approximation [Eq. (5)] but they are qualitatively identical for the second-order phase reduction case as well.)

two-dimensional system for the phase differences,

$$\gamma_{13} = \varphi_1 - \varphi_3, \qquad \gamma_{12} = \varphi_1 - \varphi_2\ . \tag{6}$$

The resulting equations represent the dynamics on a two-torus and can be studied using standard phase plane analysis techniques. In terms of the phase differences, the asynchronous state corresponds to an unbounded growth (or decline) of γ_{13} and γ_{12}. Upon increasing the coupling strength, one observes RS, wherein γ_{13} is bounded whereas γ_{12} is unbounded. For transparency and brevity, we present our theory by analyzing the first-order phase equations. Then we provide the results of the same approach applied to the second-order model.

A. Poincaré map

The transition to RS corresponds to the appearance of a stable limit cycle (LC) on the torus. Figure 2(a) depicts a typical situation for the asynchronous regime at low coupling strengths. There are no attractors on the phase plane, the motion is quasiperiodic, and the phase differences γ_{13} and γ_{12} are unbounded. Figure 2(c) exemplifies the RS state once the coupling strength increases. A stable and an unstable limit cycle are born via a saddle-node bifurcation of LCs. Note that on the LC, γ_{12} is unbounded whereas γ_{13} is bounded, which indicates the emergence of RS. Note also that we consider $\omega_1 < \omega_2$ for definiteness for the remainder of this article. Hence, the flow is from right to left. We have verified that our conclusions hold equally well for the other case.

For the following derivation, it is instructive to construct a Poincaré map, choosing the line $\gamma_{12} = 2\pi$ as the Poincaré section. A trajectory that begins on this section intersects it next at $\gamma_{12} = 0$ since the flow on the torus is leftwards. Thus, we have $\gamma_{13}(0) = P[\gamma_{13}(2\pi)]$, where $P(\cdot)$ denotes the Poincaré map. The Poincaré map corresponding to Figs. 2(a) and 2(c) are shown in Figs. 2(b) and 2(d), respectively. Evidently, RS in the system equates to a stable fixed point of the Poincaré map. We exploit this observation to derive the condition for RS analytically.

B. First-order phase dynamics

Starting with Eqs. (5), using Eq. (6), and introducing the new time $\tau = (\omega_2 - \omega_1)t$, we obtain a two-dimensional system for phase differences,

$$\begin{aligned}\gamma_{13}' &= \nu + \widetilde{\varepsilon}[-\sin\ \gamma_{12} - \alpha\ \cos\ \gamma_{12} - \sin(\gamma_{13} - \gamma_{12}) \\ &\quad + \alpha\cos(\gamma_{13} - \gamma_{12})], \\ \gamma_{12}' &= -1 + \widetilde{\varepsilon}[-2\ \sin\ \gamma_{12} - \sin(\gamma_{12} - \gamma_{13}) \\ &\quad + \alpha\ \cos(\gamma_{12} - \gamma_{13})],\end{aligned} \tag{7}$$

where

$$\nu = \frac{\omega_1 - \omega_3}{\omega_2 - \omega_1}\ , \qquad \widetilde{\varepsilon} = \frac{\varepsilon}{\omega_2 - \omega_1}\ , \tag{8}$$

and $(\cdot)'$ denotes differentiation with respect to τ.

To derive the Poincaré map $\gamma_{13}(0) = P[\gamma_{13}(2\pi)]$, we divide the preceding equations to obtain

$$\frac{d\gamma_{13}}{d\gamma_{12}} = \frac{\nu + \widetilde{\varepsilon}[-\sin\ \gamma_{12} - \alpha\ \cos\ \gamma_{12} - \sin(\gamma_{13} - \gamma_{12}) + \alpha\ \cos(\gamma_{13} - \gamma_{12})]}{-1 + \widetilde{\varepsilon}[-2\ \sin\ \gamma_{12} - \sin(\gamma_{12} - \gamma_{13}) + \alpha\ \cos(\gamma_{12} - \gamma_{13})]}. \tag{9}$$

We solve Eq. (9) with the initial condition $\gamma_{13}(2\pi)$ using a perturbation approach for which we assume the following:

$$|\omega_1 - \omega_2| \sim O(1), \qquad 0 < |\omega_1 - \omega_3| \ll 1, \qquad \varepsilon \ll 1. \tag{10}$$

Note that the first pair of assumptions formally encapsulates our previous qualitative description: The peripheral oscillators are near identical, whereas the hub oscillator is markedly different. Equivalently, in terms of the parameters present in Eq. (7), the assumptions result in $\widetilde{\varepsilon} \ll 1$ and $\nu \ll 1$.

The solution presented in Appendix A provides the condition for the existence of the Poincaré map's fixed point,

$$\left|\frac{\varepsilon^2\alpha}{(\omega_1 - \omega_3)(\omega_1 - \omega_2)}\right| \geqslant \frac{1}{2}\ . \tag{11}$$

This inequality yields the necessary condition for RS in the first-order phase reduction Eqs. (5). Its validity depends on the smallness of ε. It indicates that upon increasing the coupling strength, RS appears due to nonisochronicity. Hence, RS is impossible in a chain of three nonidentical Kuramoto equations. This result agrees with the observation reported in Ref. [3] and theoretical analysis in Ref. [6].

C. Second-order phase dynamics

Now, we use the same technique to construct the Poincaré map from the second-order phase dynamics equations. For this goal, we rewrite Eqs. (2) in terms of phase differences and then obtain an equation for $\frac{d\gamma_{13}}{d\gamma_{12}}$ that is similar to Eq. (9) but contains additional terms proportional to $\widetilde{\varepsilon}^2$. Solving this equation by the perturbation technique (see Appendix B for details), we arrive at the following condition for RS:

$$\left|\frac{\varepsilon^2[\alpha-(\omega_1-\omega_2)C_{12}]}{(\omega_1-\omega_3)(\omega_1-\omega_2)}\right| \geqslant \frac{1}{2}\,. \tag{12}$$

This condition differs from the inequality (11), derived in the first approximation by the term $(\omega_1-\omega_2)C_{12}$ alone. (Note that $C_{12}\approx C_{32}$.) This term is proportional to the amplitude of the synchronizing terms $\sin(\varphi_3-\varphi_1)$, $\sin(\varphi_1-\varphi_3)$ in Eqs. (2). These terms indicate the presence of an "invisible" coupling between oscillators 1 and 3. This coupling exists despite the absence of a physical link between the first and the third units; the first-order phase reduction does not reveal it. Thus, RS is promoted by nonisochronicity and by indirect coupling through the hub.

IV. RESULTS

To validate our derivations, we compare the bifurcation diagram on the ε-α plane obtained using the various approximations against those obtained for the exact SL equations. Before discussing the plots, we briefly recall the approximations made and clarify the terminology used to distinguish between them. The results from the numerical computations using the SL system (1) will be referred to as "exact." If the numerical calculation used the first-order [Eq. (5)] or the second-order [Eq. (2)] phase reduction, the corresponding result will be termed as "NPR1" or "NPR2," respectively [14]. Finally, the theoretical results obtained for the first-order [Eq. (11)] and second-order [Eq. (12)] phase reduction are coined as "TPR1" and "TPR2," respectively [15].

As a first step, we compared the NPR1 and TPR1 borderlines of the RS transitions. We found that TPR1 very well reproduces the numerical results shown by dashed lines in Fig. 1. This result confirms the capability of the perturbation approach to capture RS in the Kuramoto-Sakaguchi model (5).

Figure 3 presents our main result. Here, we compare the NPR2 and TPR2 borderlines of the RS transition against the exact ones. When the frequency detuning $|\omega_1-\omega_3|$ is very small as in Fig. 3(a), all borders are practically identical for low coupling strengths. As the coupling strength ε increases, the normalized coupling $\widetilde{\varepsilon}$ [see Eq. (8)] is no longer small, which causes the observed deviation between the TPR2 and NPR2 borders. Note that the NPR2 border accurately reproduces the exact RS transition throughout the considered

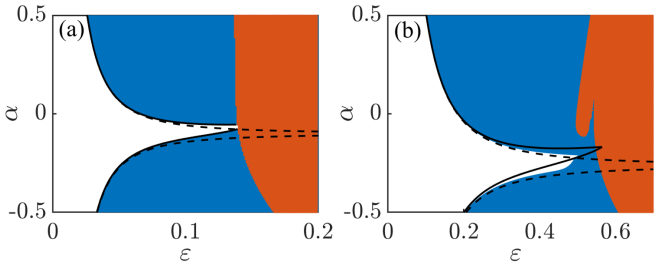

FIG. 3. Comparison of theoretical and numerical results. Two-parameter bifurcation diagrams on the ε-α plane (coupling strength versus nonisochronicity) depicting the system's state. Exact domains of RS, CS, and asynchrony are shown in blue (dark gray), red (light gray), and white, respectively. The solid black line shows the RS borderline obtained numerically using the second-order phase reduction (NPR2). The dashed black line is the corresponding theoretical solution (TPR2). The oscillators' natural frequencies are (a) $\omega_1=1,\ \omega_2=\sqrt{2},\ \omega_3=1.002$ and (b) $\omega_1=1,\ \omega_2=\sqrt{7},\ \omega_3=1.01$.

range of coupling strengths. The bifurcation diagram for a second set of natural frequencies is presented in Fig. 3(b). Again, for low coupling strengths, the agreement between the approximations and the exact solution is perfect. However, both NPR2 and TPR2 borders deviate from the exact border of the RS transition for higher values of coupling strength. This deviation occurs because ε (and likewise $\widetilde{\varepsilon}$) are no longer small quantities. We mention in passing that the dynamics for higher coupling strengths is often not trivial. For instance, the transition to CS in Fig. 3(b) near the fingerlike structure around the point $(\varepsilon=0.5,\ \alpha=0)$ exhibits complex, possibly chaotic, dynamics, presumably due to the effects of strong coupling. Interestingly, near this point, there exists a window of RS straddled by regions of CS on either side.

V. CONCLUSIONS

To summarize, we analyzed the mechanisms of RS in a chain of three SL oscillators. We demonstrated that the RS transition is determined by the interplay of the nonisochronicity and the amplitude dynamics. The impact of the latter factor renders the standard first-order phase dynamics description of the RS phenomenon invalid. Our result emphasizes the importance of higher-order phase reduction and highlights the crucial role amplitude dynamics may have in governing the behavior of networks of nonlinear oscillators.

We believe that the effect of the amplitude dynamics neglected in the first-order phase approximation and revealed by the higher-order one holds for general limit-cycle oscillators. This belief is supported by the results of numerical network reconstruction from data [16], which demonstrated the emergence of coupling between indirectly interacting units. It will be interesting to investigate how the unit's complexity may bring about qualitatively new changes to the RS transition [4,17], and if they can be explained under the present framework.

ACKNOWLEDGMENTS

M.K. was grateful for the Working Internships in Science and Engineering (WISE) scholarship by the DAAD (German Academic Exchange Service), which facilitated this work.

APPENDIX A: PERTURBATIVE SOLUTION FOR THE FIRST-ORDER PHASE APPROXIMATION

Let us assume a power series expansion for $\gamma_{13}(\gamma_{12})$ in $\widetilde{\varepsilon}$ as follows:

$$\gamma_{13}(\gamma_{12}) = \gamma_{13;0}(\gamma_{12}) + \widetilde{\varepsilon}\gamma_{13;1}(\gamma_{12}) + \widetilde{\varepsilon}^2\gamma_{13;2}(\gamma_{12}) + O(\widetilde{\varepsilon}^3). \tag{A1}$$

The next step is to substitute this expansion in Eq. (9) and gather the terms with matching powers of $\widetilde{\varepsilon}$. However, it is unclear where the terms involving ν will be grouped as the relation between ν and $\widetilde{\varepsilon}$ is unknown. This is not a problem since we may arbitrarily assume any order for ν; its correct scaling near the RS transition is found as part of the derivation by the principle of dominant balance [18]. For illustration, we have grouped ν with the $O(1)$ terms. [Alternatively, one may want to group it with $O(\widetilde{\varepsilon}^2)$ terms as that makes Eqs. (A2) shorter.] Now, we collect the terms at each order as follows:

$$\begin{aligned}
O(\widetilde{\varepsilon}^0)\text{:}\ \frac{d\gamma_{13;0}}{d\gamma_{12}} &= -\nu,\\
O(\widetilde{\varepsilon}^1)\text{:}\ \frac{d\gamma_{13;1}}{d\gamma_{12}} &= -\alpha(\nu+1)\cos(\gamma_{12}-\gamma_{13;0}) + \alpha\cos(\gamma_{12}) + 2\nu\,\sin(\gamma_{12})\\
&\quad + \nu\,\sin(\gamma_{12}-\gamma_{13;0}) + \sin(\gamma_{12}) - \sin(\gamma_2-\gamma_{13;0}),\\
O(\widetilde{\varepsilon}^2)\text{:}\ \frac{d\gamma_{13;2}}{d\gamma_{12}} &= [\alpha\,\cos(\gamma_{12}-\gamma_{13;0}) - 2\sin(\gamma_{12}) - \sin(\gamma_{12}-\gamma_{13;0})]\\
&\quad \times [-\alpha(\nu+1)\cos(\gamma_{12}-\gamma_{13;0}) + \alpha\cos(\gamma_{12})\\
&\quad + 2\nu\sin(\gamma_{12}) + \nu\sin(\gamma_{12}-\gamma_{13;0}) + \sin(\gamma_{12}) - \sin(\gamma_{12}-\gamma_{13;0})]\\
&\quad - \gamma_{13;1}[\alpha(\nu+1)\sin(\gamma_{12}-\gamma_{13;0}) + (\nu-1)\cos(\gamma_{12}-\gamma_{13;0})].
\end{aligned} \tag{A2}$$

The initial conditions associated with the differential equation of each order are as follows:

$$\gamma_{13;0}(2\pi) = \gamma_{13}(2\pi), \quad \gamma_{13;1}(2\pi) = 0, \quad \gamma_{13;2}(2\pi) = 0. \tag{A3}$$

Equations (A2) along with the initial conditions in Eqs. (A3) are solved sequentially, providing the solutions for $\gamma_{13;0}$, $\gamma_{13;1}$, and $\gamma_{13;2}$. These terms are now substituted back into the series expansion Eq. (A1). By evaluating the resultant expression at $\gamma_{12} = 0$, we arrive at a functional relation between $\gamma_{13}(2\pi)$ and $\gamma_{13}(0)$, which is the desired Poincaré map. The described procedure yields

$$\begin{aligned}
\gamma_{13}(\gamma_{12}) &= \gamma_{13;0}[\gamma_{12};\gamma_{13}(2\pi)] + \widetilde{\varepsilon}\gamma_{13;1}[\gamma_{12};\gamma_{13}(2\pi)]\\
&\quad + \widetilde{\varepsilon}^2\gamma_{13;2}[\gamma_{12};\gamma_{13}(2\pi)] + O(\widetilde{\varepsilon}^3),\\
\gamma_{13}(0) &= \gamma_{13;0}[0;\gamma_{13}(2\pi)] + \widetilde{\varepsilon}\gamma_{13;1}[0;\gamma_{13}(2\pi)]\\
&\quad + \widetilde{\varepsilon}^2\gamma_{13;2}[0;\gamma_{13}(2\pi)] + O(\widetilde{\varepsilon}^3) = P[\gamma_{13}(2\pi)],
\end{aligned} \tag{A4}$$

where the solution's dependence on the initial condition $\gamma_{13}(2\pi)$ has been explicitly pointed out using a semicolon notation.

With the expression for the Poincaré map derived, the final step involves solving for the map's fixed points. Evaluating the expression $P[\gamma_{13}(2\pi)] = \gamma_{13}(2\pi)$ leads to

$$\nu - 2\widetilde{\varepsilon}^2\alpha\,\sin[\gamma_{13}(2\pi)] + O(\widetilde{\varepsilon}\nu) = 0. \tag{A5}$$

(By the principle of dominant balance, Eq. (A5) indicates that $\nu \sim O(\widetilde{\varepsilon}^2)$. Thus, we have found the correct scaling for ν in the neighborhood of RS.) Upon neglecting the higher-order terms, the preceding equation is tantamount to

$$\sin[\gamma_{13}(2\pi)] = \frac{\nu}{2\widetilde{\varepsilon}^2\alpha}. \tag{A6}$$

For the above equation to have a solution, the absolute value of the right-hand side must be lesser than unity. This gives

$$\left|\frac{\widetilde{\varepsilon}^2\alpha}{\nu}\right| \geqslant \frac{1}{2}. \tag{A7}$$

Finally, we revert back to our original parameters ω_1, ω_2, and ε using Eq. (8) to obtain

$$\left|\frac{\varepsilon^2\alpha}{(\omega_1-\omega_3)(\omega_1-\omega_2)}\right| \geqslant \frac{1}{2}. \tag{A8}$$

APPENDIX B: PERTURBATIVE SOLUTION FOR THE SECOND-ORDER PHASE APPROXIMATION

This Appendix derives the condition for RS using the second-order phase approximation. As performed earlier, we exploit the assumptions formulated in Eq. (10). This allows us to simplify Eq. (2) as follows:

$$\begin{aligned}
\dot{\varphi}_1 &= \omega_1 + \varepsilon[\sin(\varphi_2-\varphi_1) - \alpha\cos(\varphi_2-\varphi_1)] + \varepsilon^2[D_{12}\cos(2\varphi_2-\varphi_1-\varphi_3) + C_{12}\sin(2\varphi_2-\varphi_1-\varphi_3)\\
&\quad - D_{12}\cos(\varphi_3-\varphi_1) + C_{12}\sin(\varphi_3-\varphi_1)],\\
\dot{\varphi}_2 &= \omega_2 + \varepsilon[\sin(\varphi_1-\varphi_2) - \alpha\cos(\varphi_1-\varphi_2) + \sin(\varphi_3-\varphi_2) - \alpha\cos(\varphi_3-\varphi_2)]
\end{aligned}$$

$$+\varepsilon^2[2D_{12}\cos(2\varphi_2-\varphi_1-\varphi_3)+2C_{12}\sin(2\varphi_2-\varphi_1-\varphi_3)-2D_{12}\cos(\varphi_1-\varphi_3)], \tag{B1}$$

$$\dot{\varphi}_3=\omega_3+\varepsilon[\sin(\varphi_2-\varphi_3)-\alpha\cos(\varphi_2-\varphi_3)]+\varepsilon^2[D_{12}\cos(2\varphi_2-\varphi_3-\varphi_1)+C_{12}\sin(2\varphi_2-\varphi_3-\varphi_1)$$
$$-D_{12}\cos(\varphi_1-\varphi_3)+C_{12}\sin(\varphi_1-\varphi_3)],$$

where C_{ij} and D_{ij} were defined in Eqs. (3) and (4). In particular, we have used $C_{32}\approx C_{12}$ and $D_{32}\approx D_{12}$ (up to the second order). Note the presence of terms of the form $\sin(\varphi_1-\varphi_3)$ in the first and last of Eqs. (B1), which explicitly indicate the invisible coupling between oscillators 1 and 3.

Hereafter, the procedure to derive the criteria for RS is identical to that of the first-order approximation and is not presented here for brevity. The expression obtained upon solving for the fixed points of the Poincaré map is as follows:

$$\nu-2\widetilde{\varepsilon}^2[\alpha-(\omega_1-\omega_2)C_{12}]\sin[\gamma_{13}(2\pi)]+O(\widetilde{\varepsilon}\nu)=0\ , \tag{B2}$$

which has a solution for $\gamma_{13}(2\pi)$ if

$$\left|\frac{\varepsilon^2[\alpha-(\omega_1-\omega_2)C_{12}]}{(\omega_1-\omega_3)(\omega_1-\omega_2)}\right|\geqslant\frac{1}{2}\ . \tag{B3}$$

[1] Y. Kuramoto, *Chemical Oscillations, Waves and Turbulence* (Springer, Berlin, 1984); A. Pikovsky, M. Rosenblum, and J. Kurths, *Synchronization: A Universal Concept in Nonlinear Sciences* (Cambridge University Press, Cambridge, UK, 2003); S. Strogatz, *Sync: The Emerging Science of Spontaneous Order* (Penguin, London, 2004); G. Osipov, J. Kurths, and C. Zhou, *Synchronization in Oscillatory Networks* (Springer-Verlag, Berlin/Heidelberg, 2007).

[2] K. Okuda and Y. Kuramoto, Prog. Theor. Phys. **86**, 1159 (1991)

[3] A. Bergner, M. Frasca, G. Sciuto, A. Buscarino, E. J. Ngamga, L. Fortuna, and J. Kurths, Phys. Rev. E **85**, 026208 (2012)

[4] L. Minati, Chaos **25**, 123107 (2015); B. Karakaya, L. Minati, L. V. Gambuzza, and M. Frasca, Phys. Rev. E **99**, 052301 (2019)

[5] V. Vuksanović and P. Hövel, NeuroImage **97**, 1 (2014)

[6] V. Vlasov and A. Bifone, Sci. Rep. **7**, 10403 (2017)

[7] L. V. Gambuzza, A. Cardillo, A. Fiasconaro, L. Fortuna, J. Gómez-Gardenes, and M. Frasca, Chaos **23**, 043103 (2013)

[8] H. Sakaguchi and Y. Kuramoto, Prog. Theor. Phys. **76**, 576 (1986)

[9] E. Gengel, E. Teichmann, M. Rosenblum, and A. Pikovsky, J. Phys.: Complexity **2**, 015005 (2021)

[10] Y. Qin, M. Cao, B. D. Anderson, D. S. Bassett, and F. Pasqualetti, IEEE Control Syst. Lett. **5**, 767 (2020), Y. Qin, Y. Kawano, and M. Cao, in *2018 IEEE Conference on Decision and Control (CDC)* (IEEE, 2018), pp. 5209–5214; V. Nicosia, M. Valencia, M. Chavez, A. Díaz-Guilera, and V. Latora, Phys. Rev. Lett. **110**, 174102 (2013)

[11] It is easy to check that the natural frequencies of uncoupled units equal the difference between the imaginary parts of the coefficients of linear and nonlinear terms, i.e., they are ω_n.

[12] Note that our Eq. (1) represents a particular case of a more general setup studied in Ref. [9].

[13] In the following, we always consider frequencies of the peripheral oscillators to be close whereas the frequency of the hub is essentially different.

[14] We sweep the parameter space to determine the state of the system using efficient techniques. We find RS in the SL equations (1) by looking for a limit cycle solution where γ_{12} is unbounded whereas γ_{13} is bounded using a shooting method. To detect RS using the phase reduction equations exactly, we numerically construct the Poincaré map described in Sec. III by simulating Eq. (9) (or its second-order counterpart) and check the presence of a fixed point. Regions of CS were computed using direct numerical simulations; we mark the points in the parameter space that resulted in $\Omega_1=\Omega_2=\Omega_3$ up to a tolerance of 10^{-4}.

[15] The borderline of the RS transition is given by the condition when inequalities (11) and (12) turn to equalities.

[16] B. Kralemann, A. Pikovsky, and M. Rosenblum, Chaos **21**, 025104 (2011)

[17] J. Lacerda, C. Freitas, and E. Macau, Appl. Math. Model. **69**, 453 (2019)

[18] P. D. Miller, *Applied Asymptotic Analysis* (American Mathematical Society, Providence, 2006), Vol. 75.